PSD 카메라와 프로펠라를 이용한 콘테이너 스웨이 제어

論 文
56-5-21

A New Anti Sway Control for Container Crane Using PSD Camera and Propellers

崔 然 旭* · 李 炯 基†
(Yeon Wook Choe · Hyung Ki Lee)

Abstract - The spreaders on container cranes are usually controlled to stop at the same time as their trolleys are stopped. Despite the use of adequate control systems, however, the spreaders usually have comparatively large sway movements, due to their suspension from the trolleys through cables. It is, therefore, important to accurately measure the attitudes of the spreaders, in order to suppress such sways by means of secondary control.
Until now, most of conventional anti sway control systems focus on the direct control of the movements of trolleys, which seems not suitable to speed up the entire process - loading and unloading of containers. In this paper, we suggest a new anti sway control system: By using extra equipments - two propellers to suppress the sway and a PSD camera to measure the spreader's attitude - installed on the spreader and the trolley, the sway of the suspended load is considerably suppressed. The effectiveness of the proposed scheme is verified by the computer simulation and experiment with the miniature of the container crane system.

Key Words : Container Crane, Anti-sway control, H_∞ control

1. Introduction

Overhead cranes including container cranes are widely used to transport objects in many factories, ports and work places. The fundamental motions of an overhead crane can be described as: object hoisting or lowering, trolley travel, bridge traverse. In order to increase the productivity of the system, it is necessary that all these motions of the crane should take place at high speed. This could, however, lead to undesirable sway of the suspended object if proper control action is not taken. This sway is particularly serious, because it could cause damage to the system and the surroundings. And, if the sway of the suspended object continues up to the end of the transfer then it becomes quite difficult to place the object at the final location. Therefore, it is a fundamental requirement to seek a satisfactory control method to minimize the sway during the load transfer and at the final time. Also, minimizing the time of such transfer will bring about a large cost saving.
Therefore, anti-sway and position control technology have become a requirement as a core technology for overhead crane systems and received much attention form many researchers. Until now, various control strategies have been proposed, for example, minimum-time control under a velocity constraint [1], adaptive control using dynamic feedback linearization [2], impedance control with trolley speed feedback [3] and so on. In [3], the linearization model of the the crane is used to design the controller and the observer. Recently, a new anti-sway control scheme with an acceleration sensor instead of the observer was proposed in [4~5], in which the sway angle is estimated and suppressed with the real acceleration of the trolley. Finally, there are some strategies to control using fuzzy control [6], neural network [7], non-linear control [8] and son.
Although various control methods for anti-sway and position have been proposed, most of them were focused on controlling the movement of trolleys so that the sway could be suppressed. Even though these methods show good results for diminishing the sway, it is quite difficult to speed up the loading and unloading process because it takes time for accelerating or deaccelerating the trolley while suppressing the sway. Furthermore, it seems that they cannot guarantee robustness against uncertainties of the crane's varying parameters (i. e. variation of load weight and length of rope, etc.)
In this paper, we suggest a new anti-sway and position control method for controlling a container crane which are widely used in industrial applications, especially in commercial ports. That is, by using extra equipments - two propellers to suppress the sway and a PSD camera

† 교신저자, 正會員 : 부경대학교 전기제어공학부 교수
E-mail : lhk@pknu.ac.kr
* 正 會 員 : 부경대학교 전기제어공학부 교수
接受日字 : 2006年 10月 27日
最終完了 : 2007年 2月 21日

to measure the spreader's attitude - installed on the spreader and the trolley, we are able to realize the goals of the system, namely:

(1) It stops at the desired position with the sway kept to less than the permissible value.
(2) It takes as little time as possible to make the transition from travel at a constant velocity to standstill.
(3) The robustness against parameter variations is considerably improved.

2. System Dynamics

Fig. 1 shows a general view of the container crane system. The system is composed of a trolley, cables, a PSD camera, a spreader with a container and a pair of propellers. The spreader is connected to the trolley through cables, and a pair of propellers are installed on the spreader to suppress the sway. And the PSD camera is mounted on the trolley so that it measures the sway angle of the spreader. As we understand, when the trolley is moving or stopped at a desired position without any anti-sway control, the spreader has a large sway.

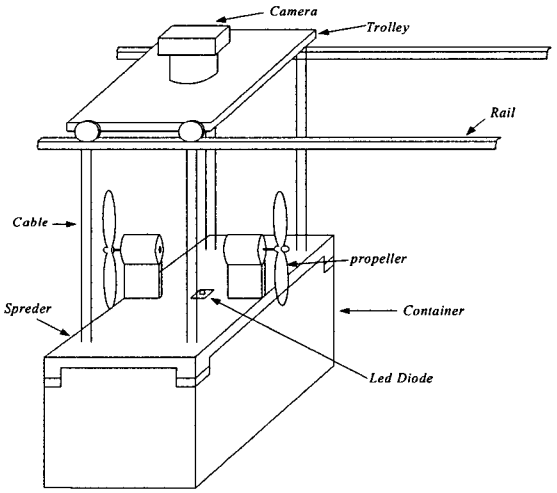

Fig. 1 A Container Crane System

Fig. 2 shows the simplified diagram of the container crane system with a suspended load (that is, spreader + container)[5]. The load, which is suspended from point O, is assumed to be a rigid body symmetric about its axial axis with mass m[kg] and center point G of mass m. The position vector of the point of suspension with respect to the fixed axes coordinated system is

$$\vec{r}_o = x\vec{i} + y\vec{j} = x\vec{i} \tag{1}$$

where $\vec{i}, \vec{j}$ are x, y directional unit vectors, respectively.

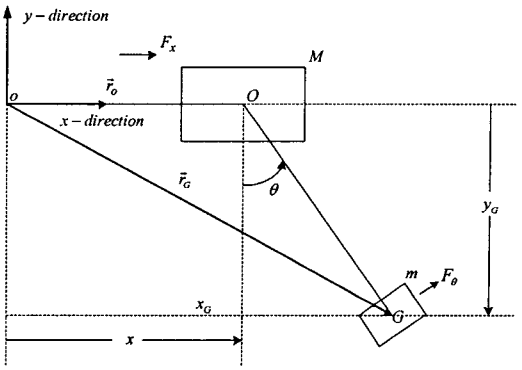

Fig. 2 Simplified diagram of the container crane system with suspended load

Using the moving circular coordinate θ to indicate the relative position of G with respect to O, the position vector of G can be written as follows

$$\vec{r}_G = x_G\vec{i} + y_G\vec{j} \tag{2}$$

where $x_G = x + l\sin\theta$, $y_G = -l\cos\theta$, and l is the length of the suspension rope and θ is the sway angle of the load. For simplicity, in this paper, the following assumptions are made:

(a) The trolley and the load can be regarded as point masses
(b) Friction force, which may exist in the moving trolley, can be neglected.
(c) Elongation of the rope due to tension force is negligible.
(d) The trolley and the load move in the xy plane, because the sway along the z-axis is negligible due to the structure.

The kinetic energy is represented by

$$\begin{aligned} T &= \frac{1}{2}M\dot{x}^2 + \frac{1}{2}m\left(\dot{x}_G^2 + \dot{y}_G^2\right) \\ &= \frac{1}{2}(M+m)\dot{x}^2 + \frac{1}{2}ml^2\dot{\theta}^2 + ml\dot{x}\dot{\theta}\cos\theta \end{aligned} \tag{3}$$

where M and m are the mass of the trolley and the load, respectively. The potential energy is also represented by

$$V = -mgl\cos\theta \tag{4}$$

where g is the gravitational acceleration. The Lagrangian function $L = T - V$ is obtained as:

$$\begin{aligned} L = &\frac{1}{2}M\dot{x}^2 + \frac{1}{2}m\left(\dot{x}^2 + \dot{l}^2 + l^2\dot{\theta}^2 + 2\dot{x}\,\dot{l}\sin\theta + 2\dot{x}\,l\dot{\theta}\cos\theta\right) \\ &+ mgl\cos\theta \end{aligned} \tag{5}$$

Now, we will use the general form of Lagrange's equation of motion:

$$\frac{d}{dt}\left(\frac{\partial L}{\partial \dot{q}}\right)-\frac{\partial L}{\partial q}=F \tag{6}$$

Eq.(6) represents the equation of motion associated with the generalized coordinates $q=[x\ \theta\ l]^T$. From the Lagrange's equation (6), the relations about the 2-directional forces are formulated as follows:

$$\frac{d}{dt}\left(\frac{\partial L}{\partial \dot{\theta}}\right)-\frac{\partial L}{\partial \theta}=F_\theta \tag{7a}$$

$$\frac{d}{dt}\left(\frac{\partial L}{\partial \dot{x}}\right)-\frac{\partial L}{\partial x}=F_x \tag{7b}$$

$$\frac{d}{dt}\left(\frac{\partial L}{\partial \dot{l}}\right)-\frac{\partial L}{\partial l}=F_l \tag{7c}$$

The force F_θ applied parallel with the swing angle θ represents the thrust of propellers, and the force F_x is applied onto the trolley according to the x direction, which is given by the amplifier connected to the motor. From Eq.(7), we easily obtain equations related to x and θ :

$$\theta:\ F_\theta\cos\theta=\ddot{x}\cos\theta+l\ddot{\theta}+2\dot{l}\dot{\theta}+g\sin\theta \tag{8a}$$

$$x:\ F_x=(M+m)\ddot{x}+ml(\ddot{\theta}\cos\theta-\dot{\theta}^2\sin\theta)$$
$$+m\ddot{l}\dot{\theta}\sin\theta+2m\dot{l}\dot{\theta}\cos\theta \tag{8b}$$

$$l:\ F_l=m\ddot{l}+m\ddot{x}\sin\theta-ml\dot{\theta}^2-mg\cos\theta \tag{8c}$$

Assume that the sway angle is sufficiently small and the hoisting and lowering velocity is made small enough that differentiation of the rope length is negligible. Then we approximately choose the values:

$$\sin\theta\approx\theta,\ \cos\theta\approx 1,\ \dot{\theta}^2\approx 0,\ \dot{l}=\ddot{l}=0 \tag{9}$$

From this, the equations of motion can be approximated as

$$\ddot{x}+l\dot{\theta}+g\theta=F_\theta \tag{10a}$$

$$(M+m)\ddot{x}+ml\ddot{\theta}=F_x \tag{10b}$$

$$m\ddot{x}\theta-mg=F_l \tag{10c}$$

where, in addition to (9), we used the relationship

$$\ddot{\theta}\cos\theta-\dot{\theta}^2\sin\theta=\frac{d}{dt}(\dot{\theta}\cos\theta) \tag{11}$$

From (10a) ~ (10c), the final form of the container crane system is given as follows:

$$\begin{cases}\ddot{\theta}(t)=-g\dfrac{(M+m)}{Ml}\theta(t)-\dfrac{1}{Ml}F_x(t)+\dfrac{(M+m)}{Ml}F_\theta(t)\\ \ddot{x}(t)=g\dfrac{m}{M}\theta(t)+\dfrac{1}{M}F_x(t)-\dfrac{m}{M}F_\theta(t)\end{cases} \tag{12}$$

Practically, however, the sway angle θ is very small value. So, (10c) can be closely approximated by $F_l=m\ddot{x}\theta-mg\approx-mg$. This suggests that the hoist motion is decoupled from the trolley[5].

From (12), we have a state-space equation for designing a controller by choosing the state vector and input as $\vec{x}(t)=[x\ \dot{x}\ \theta\ \dot{\theta}]^T$ and $\vec{u}(t)=[F_x\ F_\theta]^T$:

$$\begin{cases}\dot{\vec{x}}(t)=A\vec{x}(t)+B\vec{u}(t)\\ \vec{y}(t)=C\vec{x}(t)\end{cases} \tag{13}$$

where

$$A=\begin{bmatrix}0&1&0&0\\0&0&gm/M&0\\0&0&0&1\\0&0&-g(M+m)/Ml&0\end{bmatrix},\ B=\begin{bmatrix}0&0\\1/M&-m/M\\0&0\\-1/Ml&(M+m)/Ml\end{bmatrix} \tag{14}$$

$$C=\begin{bmatrix}1&0&0&0\\0&0&1&0\end{bmatrix}$$

3. Control System Design

3.1 Determination of the thrust of propellers

The details of propeller propulsion are very complex because the propeller is like a rotating wing. Propellers usually have between 2 and 6 blades (we used 2 blades) and various kinds of shapes (for example, thickness, length, angle of twist). These variations make analyzing the airflow through the propeller a very difficult task. Therefore, we derive a simple equation between the input voltage and the thrust under some assumption, that is, the spinning propellers act like a disk through which the surrounding air passes.

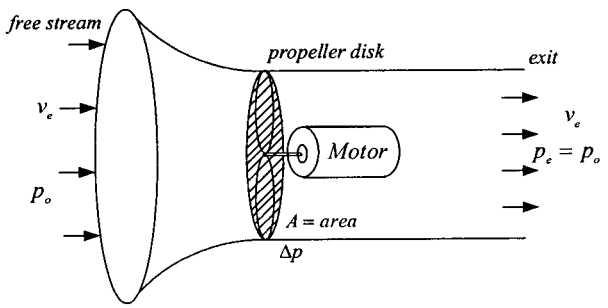

Fig. 3 Determine the thrust of the propeller

The DC-motor turns the propeller and does work on the airflow. So there is an abrupt change in pressure across the propeller disk. From the airfoil theory, we know that the pressure over the top of a lifting wing is lower than the pressure below the wing. By applying Bernoulli's equation to the air in front of the propeller and to the air behind the propeller as follows[8]:

The thrust F generated by the propeller disk is equal to the pressure jump Δp times the propeller disk area A :

$$F=\Delta p \cdot A \tag{15}$$

We can use Bernoulli's equation to relate the pressure and velocity ahead of and behind the propeller disk, not through the disk. Ahead of the disk the total pressure pt_o equals the static pressure p_o plus the dynamic pressure $0.5 r V_o^2$. That is

$$pt_o = p_o + 0.5 r V_o^2 \tag{16}$$

where $r = 1.2045\ [\mathrm{Kg/m^3}]$ is the standard air density and V_o is the velocity of air inhalation. Behind the disk,

$$pt_e = p_o + 0.5 r V_e^2 \tag{17}$$

where pt_e is the downstream total pressure and V_e is the exit velocity of air. At the disk itself the pressure jumps

$$\Delta p = pt_e - pt_o = 0.5 r \left(V_e^2 - V_o^2 \right) \tag{18}$$

Substituting Eq.(18) into Eq.(15), we obtain

$$F = 0.5 r A \left(V_e^2 - V_o^2 \right) \tag{19}$$

By the way, because the velocity of air inhalation V_o generally represents the velocity of a moving object with propellers, we neglect this in the experiment.[1] And the magnitude of the exit velocity V_e is determined experimentally, by which the thrust F can be obtained as a function of the input voltage.

3.2 The Generalized Plant for H_∞ Design

Let us consider a generalized plant shown in Fig. 4, in order to design a control system which is robust against disturbance and parameter variations(that is, uncertainty).

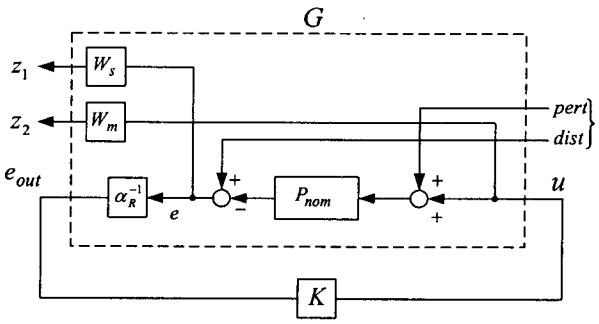

Fig. 4 The Generalized Plant for H_∞ controller Design

In Fig. 4, P_{nom} is the nominal plant, K is the controller, W_m and W_s are the weighting functions for model uncertainty[2] and output sensitivity, respectively. And $dist$ is the disturbance input, z_1 and z_2 are the fictitious outputs for H_∞ controller design, and α_R^{-1} is a variable parameter, by which robust performance against disturbance is determined. Finally, input $pert$ (and output z_2) is used for describing plant uncertainty[9~10].

It is known that the weighting functions, especially W_m related to the nominal model uncertainties, play an important role in the robust controller design. In this paper, the weighting W_m is determined as follows:

It seems suitable that the model uncertainty is mainly caused by the variation of the weight of the suspended load (that is, a container), we adopt the multiplicative uncertainty at the input side of the plant. That is, after varying the weight of the load m within the range of 10% ~ 100%, the weighting function W_m is determined by checking every possible function satisfying

$$\left| P_{nom}^{-1}(j\omega) \left(\tilde{P}(j\omega) - P_{nom}(j\omega) \right) \right| \le \left| W_m(j\omega) \right| \tag{20}$$

where $\tilde{P}(j\omega)$ is the computed frequency response obtained under the variation of the parameter m within the given range.

From Fig. 4, the generalized plant G can be expressed by

$$G = \begin{bmatrix} W_s P_{nom} & W_s & W_s P_{nom} \\ 0 & 0 & W_m \\ \alpha_R^{-1} P_{nom} & \alpha_R^{-1} & \alpha_R^{-1} P_{nom} \end{bmatrix} \tag{21}$$

and the relation between input and output is

$$\begin{bmatrix} z_1 \\ z_2 \\ e_{out} \end{bmatrix} = G \begin{bmatrix} pert \\ dist \\ u \end{bmatrix} \tag{22}$$

1) In this case, because V_o represents the speed of the moving spreader, so $V_e \gg V_o$.

2) In this case, we adopted input multiplicative perturbation uncertainty.

Using these relationships, the H_∞ control method is applied to compute a controller which satisfies

(S1) K stabilizes G
(S2) $\| T_{zw} \|_\infty < \gamma$

where T_{zw} denotes the transfer function form $w = [pert\ \ dist]^T$ to $z = [z_1\ z_2]^T$. There are several methods to obtain a robust controller which meets (S1) and (S2) requirements, for example, Loop shaping and LMI (Linear Matrix inequality). We choose LMI method because it relaxes various conditions absolutely indispensable to the other methods[11]. The obtained controller and weighting functions used in Fig. 4 are shown in the appendix.

4. Simulation and Experimental Results

First, we check the appropriateness of the generalized plant of Fig. 4 by simulation, and confirm the effectiveness of the obtained controller through experiment.

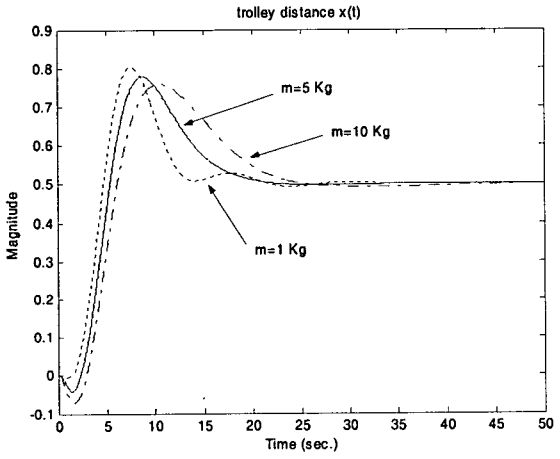

Fig. 5 (a) Response of H_∞ controller (distance of trolley)

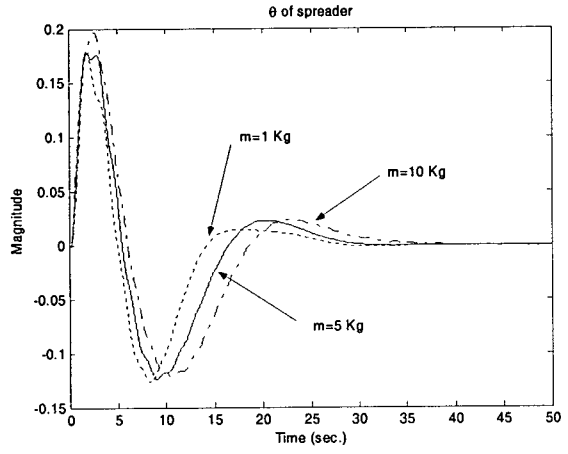

Fig. 5 (b) Response of H_∞ controller (sway angle of load)

4.1 Simulation Results

We, at first, increased the weight of load from 1[kg] to 10[kg] (nominal value, 5 [kg]) incrementally and check the output, that is, the distance of the trolley $x(t)$ [m] and the sway angle of the load $\theta(t)$ [rad]. Fig. 5 (a), (b) show results of simulation. From the figure, it is well-known that the distance of the trolley settles down its desired position despite of parameter variation, and the sway angle becomes zero with the lapse of time. It, however, takes comparatively a little longer to settle down to zero. Fig. 6 shows the inputs, that is, the input to the trolley and propeller, from which we know that the anti-sway controller works quite well in spite of large parameter variations.

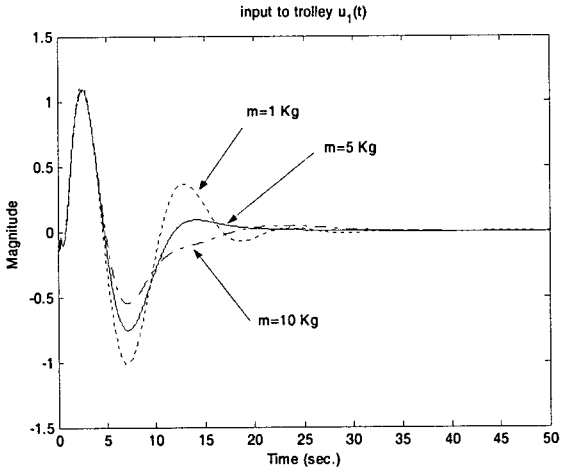

Fig. 6 (a) Input to trolley

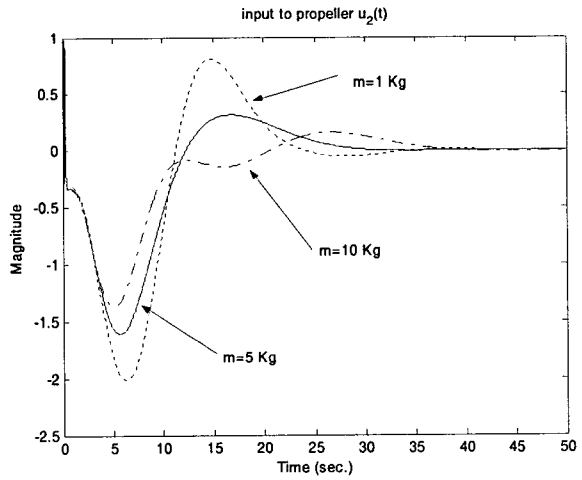

Fig. 6 (b) Input to propeller

4.2 Experimental Results

To confirm the effectiveness of the proposed scheme, some experiments have been performed with a miniature of the container crane system (Fig. 7). Fig. 8 shows the entire block diagram for controlling sway of the spreader

of the container crane system. The trolley has a 10-turn potentiometer to get the information of its position and velocity, and a PSD camera is mounted on the trolley to measure the sway angle of the spreader. The output of the control board (PC) is applied to DC-motor and BLDC motor driver through 12 bit D/A converter. The parameters of the experimental system are represented in Table 1.

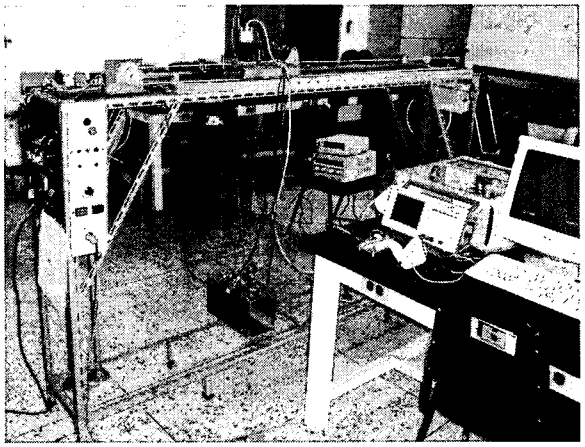

Fig. 7 Experimental Setup

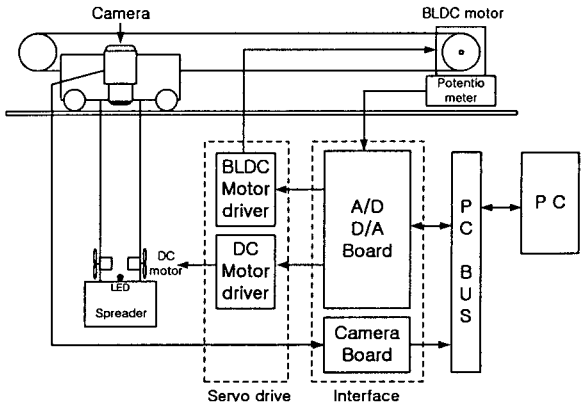

Fig. 8 Block Diagram of the experimental system

Table 1 Experimental parameters

Parameters	Value	Unit
Sensitivity of camera	26	Ωm
Focal length	85	mm
Number of resolution	2048	Pixel
Weight of trolley	2.7	kg
Weight of spreader	1	kg
Length of rope	0.91	m
Gravitational acceleration	9.8	m/s^2

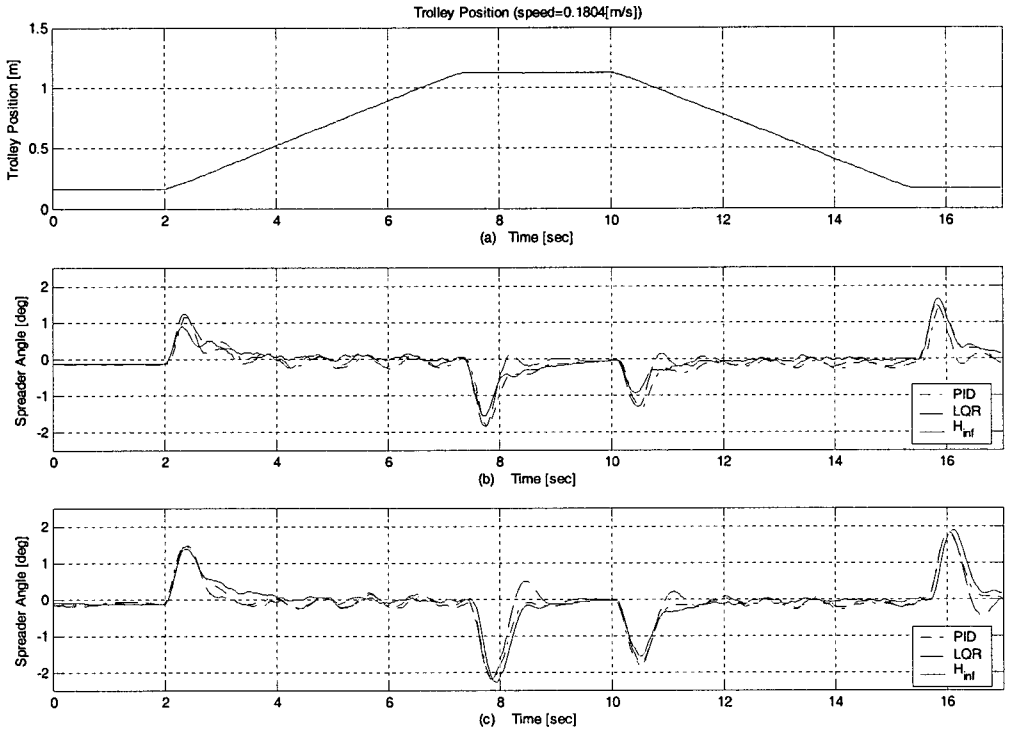

Fig. 9 Trolley Position and Sway-angle of spreader
(a) Trolley Position, (b) Sway-angle of spreader (1kg), (c) Sway-angle of spreader (5kg)

To verify the performance of the proposed anti-sway control scheme with the PSD camera and propellers, experiments are carried out under various load conditions, that is, the weight of the container in the experimental setup of Fig. 7. And to compare the effectiveness of the proposed control scheme, we adopted two extra controllers designed by using PID and LQR methods which are common for industrial applications.

Fig. 9 gives the experimental results concerning the sway angle when the trolley is moved to the target location, then come back to the original position: (a) is the trolley position when it moves at a speed of 0.18[m/s], (b) and (c) represent sway angle of the spreader without and with a load (2.5kg), respectively. It can be seen from Fig. 9 that the sway angle of the spreader settles down to (almost) zero within the reasonable time span despite of parameter variations. Since the reasonable target performance in the experiment is that the error on the sway angle is within ± 0.02 rad([5],[6]), the proposed control system seems to satisfy the target performance. Thus, the proposed structure with a PSD camera and propellers is quite effective in suppressing the sway. Among three controllers, the one used in the paper shows the better results in the respect of suppressing the sway angle, although it shows a little overshoot when the trolley begins to start.

Fig. 10 shows the sway-angle of the spreader when disturbance enters the system, that is, a high wind from a fan is added directly to the spreader. From the figure, the sway-angle seems well-suppressed even though there remains a small shake.

5. Conclusion

In this paper, a new scheme is proposed to control the sway of the suspended load of the container crane system. The proposed scheme, which shows comparatively good results although making direct comparisons with conventional methods haven't been performed, controls directly the sway angle using a couple of propellers and a PSD camera mounted on the trolley. The feasibility of the proposed method has been verified through simulation and experiment. From the experimental results, we certify the performance of the proposed control system.

In order to apply this method to commercial crane systems, it requires that finding out the exact relationships between the thrust of propellers and applied inputs be found, and the effect of the propellers' gust to the entire system be also thoroughly examined.

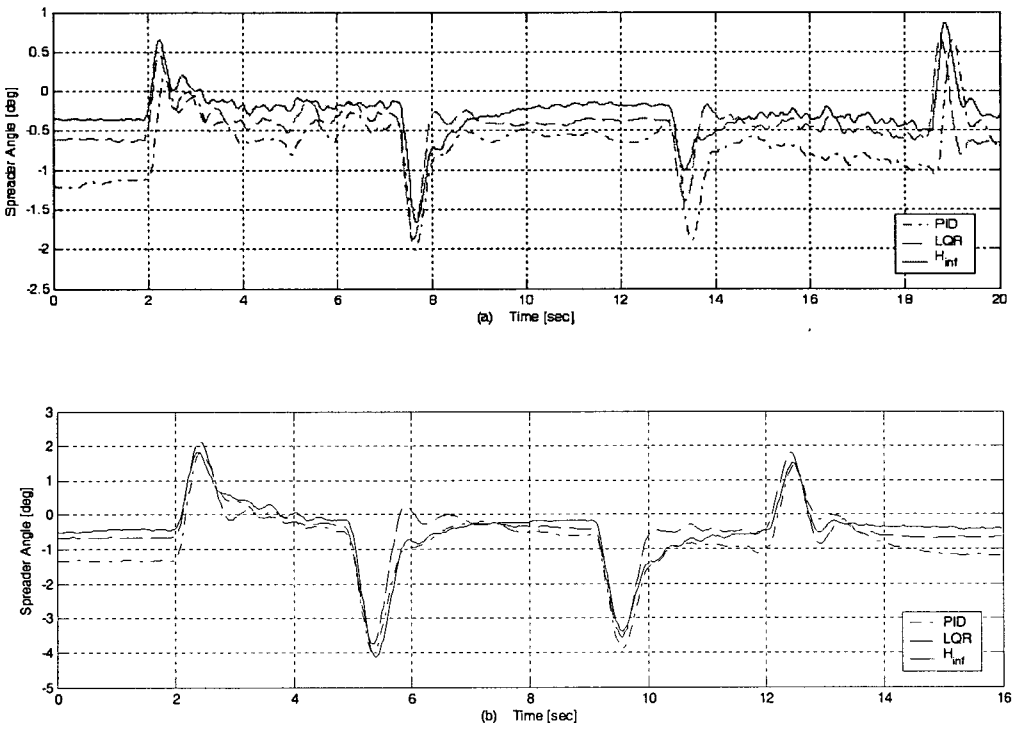

Fig. 10 Sway-angle of spreader under disturbance
(a) without container (1kg), (b) with container (5kg)

6. References

[1] T. Mita and T. Kanai, "Optimal control of the crane system using the maximum speed of the trolleys," Trans. Soc. Instr. Control Eng., 15, pp.833-838, 1979

[2] F. Boustany and B. d'Andrea-Novel, "Adaptive Control of an Overhead Crane using Dynamic Feedback Linearization and Estimation Design," Proc. of IEEE Int. Conf. on Robotics and Automation, pp.1963-1968, 1992

[3] Y. Hakamada and M. Nomura, "Anti-sway and Position Control of Crane System," AMC'96 -MIE, pp.657-662, 1996.

[4] Y. Kim, H. Seo, and S.K. Sul, "A New Anti-Sway Control Scheme for Trolley Crane System," 36th IEEE Conf. on Industry Applications, pp.548-552, 2001

[5] Y. Kim, H. Shim, H. Yoshimura, N. Fujioka, and H. Kasahara, "A New Vision-Sensorless Anti-Sway Control System for Container Cranes," 38th IEEE Conf. on Industry Applications, pp.262-269, 2003

[6] M. Gutierrez and R. Soto, "Fuzzy Control of a Scale Prototype Overhead Crane," Proc. of IEEE Conf. on Decision & Control, pp.4266-4268, 1998

[7] J.A. Mendez, L. Acosta, L. Moreno, A Hamilton and G.N. Marichal, "Design of a Neural Network Based Self-Tuning Controller for an Overhead Crane," Proc. of IEEE Int. Conf. on Control Applications, pp.168-171, 1998

[8] H. Alli and T. Singh, "Passive Control of Overhead Cranes," Proc. Of IEEE Int. Conf. on Control Applications, pp. 1046-1050, 1998

[9] J.C. Doyle, B.A. Francis and A.R. Tannenbaum, Feedback Control Theory, Maxwell MacMillan, 1992.

[10] K. Zbou, Robust and Optimal Control, Chap. 9, Prentice-Hall, 1996

[11] C. Scherer & M. Chilali, "Multiobjective Output-Feedback Control via LMI Optimization," IEEE Trans. Auto. Contr., Vol. AC-42, no.2 pp. 896-911 (1997)

Appendix 1.

1) The weighting functions used in Fig. 4 are as follows:

$$w_m = \frac{1.083s^3 + 5.668s^2 + 10.465s + 6.651}{s^3 + 1.199s^2 + 15.665s + 16.85}$$

$$\rightarrow W_m = \mathrm{diag}[w_m, w_m]$$

$$w_s = \frac{13.298}{9.947s + 1} \quad \rightarrow W_s = \mathrm{diag}[1, w_s]$$

2) Since the order of the controller which was originally computed by LMI method is too high (that is, 13), we adopted a model reduction method in order to reduce the order of the controller. The final controller which was used in the experiment is as follows:

$$K = \left[\begin{array}{c:c} A & B \\ \hdashline C & D \end{array}\right]$$

$$= \left[\begin{array}{cccc:cc} -4.8e+2 & 8.9e+2 & -8.5e+1 & -3.5e+2 & -1.4e+3 & -1.2e+3 \\ -9.6e+2 & -2.1e+3 & 8.7e+2 & 8.1e+2 & 1.1e+3 & 5.8e+3 \\ 0 & 0 & -4.1e+2 & -6.0e+2 & -8.3e+2 & -2.5e+3 \\ 0 & 0 & 0 & -2.7e+2 & -1.1e+3 & 2.4e+3 \\ \hdashline -3.3e+0 & 3.5e+3 & -3.7e+3 & -2.6e+3 & 1.1e+3 & -6.6e+2 \\ 4.5e+2 & 4.3e+3 & -8.2e+2 & -2.0e+2 & -1.1e+3 & 6.5e+2 \end{array}\right]$$

Acknowledgement

This work was supported by Pukyong National University Research Fund in 2005 (PK-2005-045)

저 자 소 개

최 연 욱 (崔 然 旭)

Yeon-Wook Choe was born in Busan, Korea, in 1955. He received the B.S. and M.S. degrees from Hanyang University, Korea, in 1978 and 1980, respectively, and Ph.D. degree in control engineering from Kyoto University, Japan, in 1990. From 2002 to 2003 he was a visiting researcher at the Univ. of Iowa, U.S.A. Since 1990, he has been with the department of control & Automation at Pukypong National Univ., Korea. His current research interests are system identification for control, control system design, and sampled-data control theory.

Tel : 051-620-1633

Fax : 051-623-4227

E-mail : wook@pknu.ac.kr

이 형 기 (李 炯 基)

Hyung-Ki Lee was born in Busan, Korea, in 1951. He received the B.S., M.S. and Ph.D. degrees from Dong-A University, Korea, in 1975, 1980, and 1984, respectively. Since 1982, he is working for the department of control and Automation of Pukyong National University. His main research area is system control with application to industrial area, and control system design with various application tools.